



Manufacture of low fume welding electrode using synthetic rutile flux material

Rahul Madhusoodhanan¹ · Sivapirakasam Suthangathan Paramashivan¹ · Sreejith Mohan¹ · Vishnu B. Rajeshwari² · Guruvayurappan Murali¹

Received: 2 October 2021 / Accepted: 20 July 2022 / Published online: 10 August 2022
© The Author(s), under exclusive licence to Springer-Verlag London Ltd., part of Springer Nature 2022

Abstract

This paper presents the influence of synthetic rutile addition to the electrode flux on the shielded metal arc welding emissions. A systematic study was conducted by modifying the electrode flux composition with synthetic and conventional rutile combinations. The fume particulates emitted during welding were sampled using an AWS F1.2 standard fume test chamber, and its concentration was determined through gravimetric analysis. Online monitoring of arc stability, droplet transfer characteristics, and spatter formations was performed using digital storage oscilloscope, high-speed camera, and infrared camera devices, respectively. The UVC and ozone concentrations in the arc atmosphere were also measured using standard procedures. The results revealed that the addition of synthetic rutile up to 50% could reduce the fume emissions by as much as 31.4% compared to the conventional electrode. The present study also focused on the reduction of hexavalent chromium (Cr(VI)), a hazardous and carcinogenic chemical species in welding fumes. In order to achieve a combined reduction in the concentration of hexavalent chromium and fume, Zn, a reactive metal, was added to the electrode flux of the experimental electrodes. The primary mechanism of reduction in fumes and Cr(VI) concentration was recognized from the study as the decrease in the surface tension of the pendent liquid droplet ensued by the presence of fine-grained TiO₂ in the synthetic rutile. Apart from lowering fume emissions, the experimental electrodes achieved a deposition efficiency of up to 61.9%, which was appreciably higher than that of the conventional electrode.

Keywords Welding fume · Synthetic rutile · Hexavalent chromium concentration · Arc stability · Surface tension · Ozone concentration · Weld chemistry · Deposition efficiency · Delta quantity · Droplet diameter · Spatter formation

1 Introduction

Welding is one among the effective methods for joining metallic modules. It is estimated that roughly 3 million working population across the world is involved in welding and its allied jobs [1]. The most commonly employed method of all the welding processes is shielded metal arc welding (SMAW). Many types of SMAW electrodes are being manufactured, and depending on the main constituent of their flux, they are grouped into three categories:

rutile, basic, and cellulosic coating materials. Rutile-based electrode is the most commonly employed and considered to be the most welder-friendly flux because of its excellent control properties on the arc stability and hence its better weldment [2]. Among the rutile-based welding electrodes, the primary arc-stabilizing material is natural rutile (TiO₂), which constitutes about 40–48% by weight of the electrode flux. However, due to its higher cost and growing concern on its long-term availability, in the recent past, there is an impetus to find a potential substitute for it, hence the development of synthetic rutile [3]. Synthetic rutile which contains 96% TiO₂ content is normally obtained normally through a chemical treatment method from a naturally occurring ore, so-called ilmenite (FeTiO₃) [4, 5]. The mines and reserves of ilmenite in the world are found abundant and surpassed natural rutile.

Chen et al. [6] reported that synthetic rutile could be a possible replacement material for natural rutile in the welding electrode flux owing to its excellent mechanical

✉ Sivapirakasam Suthangathan Paramashivan
spshivam@nitt.edu

¹ Industrial Safety Engineering Lab, Department of Mechanical Engineering, National Institute of Technology, Tiruchirappalli, India

² Department of Mechanical Engineering, Marian Engineering College, Thiruvananthapuram, Kerala, India

and thermal properties. While natural rutile has a granular structure composed of single crystals, synthetic rutile concentrates are in the form of ultra-fine crystals ensuing potential advantages in terms of its chemical reactivity in the welding arc. Yet, prior to recommending synthetic rutile as a substitute for natural rutile in the welding flux, its effect on tailoring the hazardous emissions from welding such as emission of toxic metallic fumes, ultraviolet (UV) radiation, ozone concentration, and hexavalent chromium in fumes need to be addressed.

There are quite a lot of studies reported on the characterization and mitigation of fumes from a SMAW process. However, a breakthrough in this study happened when it was realized that arc-stabilizing materials in the welding electrode flux such as Al_2O_3 and TiO_2 gave a better performance in their nanostructured form. This was first proved by Sivapirakasam et al. [7] where the authors introduced the nano-sized Al_2O_3 on core welding wires prior to flux coating and reduced the fume concentration without any adverse effect on the weld quality. The authors confirmed that nano-alumina participated in ionization reactions and improved the stability of the arc atmosphere, thereby having reduced fume levels.

Another report by Mohan et al. [8] indicated the favorable influence of introducing nanostructured TiO_2 on the electrode wire on reducing the welding fume concentration. Later, Sivapirakasam et al. [9] deposited nano-aluminum oxide and titanium dioxide coating on stainless steel welding wires and studied its effect on the concentration of hexavalent chromium (Cr(VI)), a potential carcinogen for humans, in welding fumes. Intriguingly, the authors noted a trade-off between the generation rates of fume and hexavalent chromium concentration.

Vishnu et al. [10] developed a method for concurrently reducing fume and hexavalent chromium by utilizing multi-layered nanostructured Al_2O_3 and TiO_2 for fume mitigation and as tertiary material ZnO for Cr(VI) reduction. In a subsequent investigation, the scientists found a drop-in fumes and Cr(VI) concentrations when micro-sized CaCO_3 was replaced with its nano-sized counterpart in the welding flux. However, the research on control of fumes and its hazardous constituents from a SMAW process is still premature and needs further development.

Other than fumes, welders are also exposed to hazardous UV radiation and ozone whose formations in the weld atmosphere are essentially interrelated. Ozone is generated

through the reaction of UVC radiation and oxygen in the welding atmosphere [10–13]. Ozone, being an irritant gas, has detrimental effects on the skin, mucous membrane, and throat of the welder. When ozone reaches the lungs, it reduces the rate of pulmonary ventilation and lower the generation of CO_2 . Besides, ozone is actually not a very stable compound, and it converts chromium from its lower oxidation state to Cr(VI) in welding fume due to this strong oxidation property. Thus, it is apparent that, in order to curtail the Cr(VI) concentration, it is required to control the generation of ozone and UVC radiation from welding. However, no such studies for a SMAW process reported till date.

The objective of this paper is to characterize the impact of replacing natural rutile with synthetic rutile in the welding electrode flux on the hazardous fume emissions in an occupational environment. In order to check the efficacy of the addition of synthetic rutile and to address the uncertainty in fully replacing natural rutile with synthetic rutile, its concentration was varied in definite proportions in the welding electrode flux. As a concurrent method for the combined reduction of fume formation rate and hexavalent chromium concentration, Zn, a reactive metal, was also incorporated into the electrode flux. Ozone and UVC concentrations in the arc atmosphere, chemical compositions of fume, and elemental deposition are also reported. The proposed knowhow of substituting natural rutile with synthetic in the electrode welding flux is expected to be an effective technique for the welding electrode manufacturing in the future.

2 Experimental procedure

2.1 Welding

Welding was carried out on a SS316L circular plate of 360 mm diameter and 12 mm thickness. The electrode employed was E316 L of the dimension 350 mm × 4 mm [14]. Table 1 shows the chemical composition of the base metal and the core welding wire. The flux chemistry of E316 L, as given by the electrode manufacturer (Logos Weld Products), is given in Table 2. The experimental electrodes E1, E2, E3, and E4 were prepared by substituting the natural rutile in the conventional electrode flux with TiO_2 -enriched synthetic rutile in definite proportion by weight of 25%, 50%, 75%, and 100% in that order. Fixed concentration (1% by weight) of Zn was added to each electrode flux with the

Table 1 Base metal and core wire chemical composition

	Element (wt%)									
	Mn	Mo	Ni	Cr	S	Si	N	P	C	Fe
Base metal	1.5–2	1.8–3.5	9–14	14.5–18.5	0.02	1	0.12	0.045	0.03	Bal
Core wire	1–2	1.5–5.5	8–13	4.5–19.5	0.03	1.2	0.12	0.050	0.02	Bal

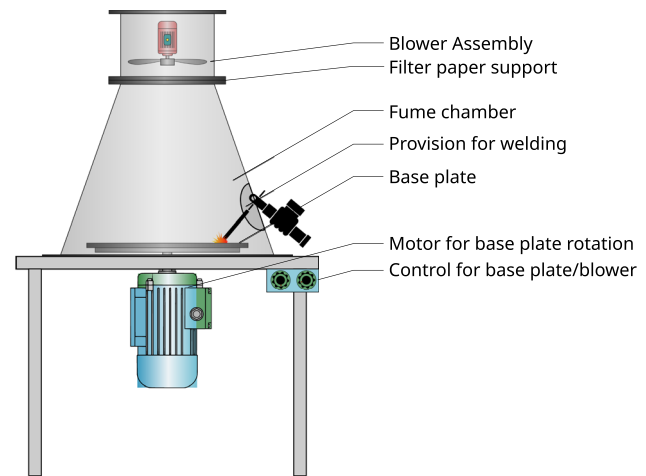
Table 2 Flux chemical composition

Chemical component	Composition (% by weight)
Rutile	22–52
Titanium oxide	10–15
Sodium silicate	1–5
Ferro silicon	0.1–1
Calcium carbonate	15–18
Chromium	15–25
Nickel	3–9
Ferro manganese	1–3
Molybdenum	0–4
Calcium fluoride	2–10
Cryolite	0–5
Field spar	0–3
Niobium	0–3
Potassium titanate	0–3
Chromium(III) oxide	0–0.5
Potassium silicate	1–5
Potassium hydroxide	0–0.5

aim of reducing Cr(VI) concentration in welding fume. All the electrodes were produced using an electrode manufacturing setup (make: Logos, model: EP 50) through a sequence of operations, namely dry mixing, wet mixing, slug pressing, extrusion, and baking under identical conditions. For measuring the density of conventional and experimental electrode flux formulations, the 10 mL volume of powder specimens measured using a standard cylindrical flask was gravimetrically weighed using a precision weighing balance (precision: 0.01 g, make: Metis, model: 007). The chemical compositions of the synthetic and natural rutilites were tested using X-ray fluorescence spectroscopy (precision: 0.1%, make: Panalytical, model: PW4400/40) [15–17].

2.2 Fume formation rate, arc stability, and droplet transfer

The fume formation rate (FFR) was determined by sampling welding fumes in an AWS F1.2 standard fume test chamber [18, 19]; the test chamber's schematic diagram is depicted in Fig. 1. The base plate was cleaned with a wire brush prior to welding to remove any contaminants. A constant current power source of an inverter type ARC/TIG welding machine (make: Rilox, model: TIG 200) was employed for welding. The electrode used in the study was having the dimension of 350 mm length \times 4 mm diameter, with a permissible current range of 110–150 A and a voltage of 5–50 V. In order to effectively profile the fume emission from the electrode, a higher set current of 140

**Fig. 1** Schematic of the AWS F1.2 standard fume test chamber

A was used. Welding was carried out for 60 s, and the extractor fan was let operational for 90 s more in order to achieve higher fume collection efficiency.

An experienced welder deposited bead on plate welds on the revolving base plate while maintaining a draw angle of 15°–30°. Consistent welding speed and feed rate of 15 cm/min and 18 cm/min, respectively, were maintained throughout the process. During 60 s of welding, fumes were collected on a glass microfiber filter paper (253 mm \times 204 mm and 1.6- μ m pores) at a flow rate of 900 L/min.

The FFR was determined gravimetrically using a dynamic high-precision weighing balance (accuracy 0.1 mg, precision ≤ 0.1 mg/ ≤ 0.05 mg, make: Shimadzu, model: AUW220D). The mass concentration of fumes was estimated from the weight difference of the filter paper prior to and after sampling as per the following equation (Eq. (1)):

$$\text{Fume formation rate (FFR)} = \frac{F_w - I_w}{t} \text{ g/min} \quad (1)$$

where I_w is the initial weight of filter paper, F_w is the final weight of filter paper, and t is the time taken for welding. The fume collection and measurement were carried out in triplicate for each type of electrode, and an average value of FFR was recorded in the study.

The filter paper was then digested and extracted in accordance with the NIOSH 7300 standard, and the individual metallic constituents in fumes such as Ti, Ni, Si, Fe, Mo, Cr, and Mn were determined using the inductively coupled plasma atomic emission spectroscopy (ICP-AES) (precision: 3.3–7.7%, make: PerkinElmer, model: Optima 5300DV).

The arc stability during welding was determined using an online measurement of the probability density of arc voltage. Arc voltage and current data were collected and analyzed

using a digital storage oscilloscope (DSO) instrument (precision: 0.05/time per div, make: Agilent Technologies, model: DSO7054B). A differential probe was used to detect the voltage, while the current was monitored using a current probe of clamp type (precision: 500 μ A, make: Chauvin Arnoux, model: PAC12) (1 mV/A and 10 mV/A). Another technique for measuring arc stability was to use an infrared camera to capture the spatters produced during welding (make: Flir; model: SC7500-MB). The lens employed had a focal length of 25 mm, and the camera was kept near to the weld zone at a distance of approximately 1 m.

The dynamic behavior of the molten droplet transfer from the electrode was visualized using a high-speed camera (make: Photron, Fastcam model: 775 K-M1). The video was shot at 7000 frames per s and resolution of 700 \times 400 pixels. Cavitar Cavilux HF illumination system was used for enabling clear visualization of welding processes as if they were essentially cold by eliminating welding brightness.

2.3 Cr(VI) formation rate, UVC, and ozone concentrations

Concentration of Cr(VI) in welding fumes was measured following the NIOSH 7600 standard. Accordingly, the filter paper was digested in a solution of 2% NaOH-3% Na₂CO₃ and subjected to analysis in a UV-visible spectrophotometer (precision: \pm 2 nm, make: Shimadzu, model: UV-2600) at a wavelength of 540 nm. The analysis gave the weight percentage of Cr(VI) in welding fumes which is then expressed as hexavalent chromium formation rate.

UVC emission from the welding source was identified using a UV light meter (precision: 0.01 mw/cm², make: Lutron Electronic, model: YK-37UVSD) capable of capturing UV radiation in the range of 200–280 nm. The detector head of the UV meter was attached to a mechanical system as shown in Fig. 2 and positioned at an angle of 15° from the center of the arc facing it [20]. The effective irradiance of UVC was measured at a distance of 1 m from the center of arc. An average of three replicates was taken, and the percentage error was found to be \pm 10%.

The concentration of ozone produced during welding was determined using a UV absorption ozone analyzer (precision: 0.001 ppm, make: Faraday Ozone, model: OA-964). Figure 2 gives the schematic illustration of the experimental method. Using the analyzer, the concentration of ozone could be measured within 0–5000 parts per billion (ppb) in a 0.5-s response time. The analyzer's inlet probe was angled 60° away from the arc's center and 1 m distant from it to ensure optimal collection efficiency. The probe was linked to the analyzer through a polytetrafluoroethylene (PTFE) tube with a 37 mm diameter and a 0.5-m PTFE filter to prevent welding fume from entering the ozone analyzer. Prior to the start of the studies, the sample probe, connecting tube, and filter were conditioned for 10 min with ozone generated by an ozone generator [21, 22]. The ozone concentration was averaged during a 60-s period following the initial welding.

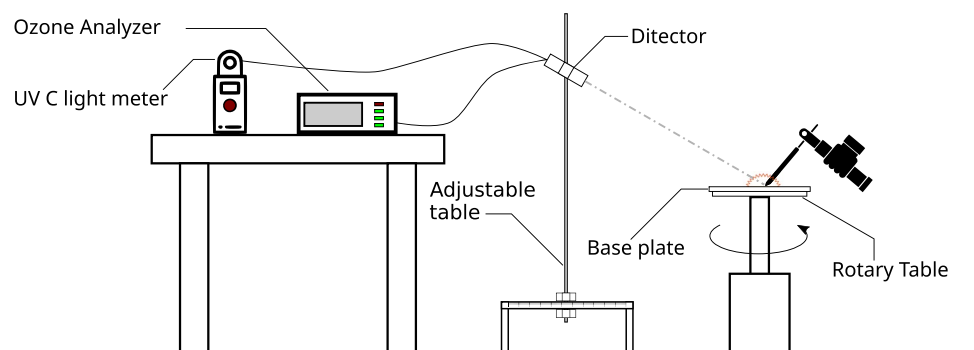
In general, UVC and ozone measurements can be influenced by the ambient conditions of the test environment. However, during the measurements, utmost care was taken in order to eliminate such disturbances. All the measurements were carried out under controlled test room conditions. The room dimensions were 3.04 m \times 3.04 m \times 2.74 m with a small ventilation of size 0.60 m \times 0.30 m, and there were no source of UVC and ozone. While measuring the UVC and ozone concentrations, the door was kept closed in order to avoid external influences.

2.4 Weld chemistry and delta quantity

For elemental measurements of alloying elements in the weld such as Cr, Mn, Fe, Ni, Mo, Si, and Ti, a tube-based portable hand-held X-ray fluorescence (XRF) device (precision: 0.1%, make: S1 Titan, model: 800) was used [23]. Prior to measurements, good brushing to clean off the weld spatter, scaling, and rust was carried out by using a wire brush. It is essential to take a minimum of 3 tests across the welded area to get more accuracy of the result.

The loss of elements during the welding process via transfer from the weld metal to the slag contributes to fumes

Fig. 2 Schematic of UVC and ozone measuring apparatus



by its evaporation [24, 25]. This elemental transfer can be calculated using the element's delta quantity (Eq. (2)) which is shown below:

$$\Delta \text{ Quantity} = \text{Analytical composition} - \text{Nominal composition} \quad (2)$$

The nominal composition can be calculated from the following relation:

$$\frac{\text{Dilution} \times \text{Baseplate composition} + (100 - \text{Dilution}) \times \text{Wire composition}}{100}$$

The analytical composition, on the other hand, refers to the weight fraction of each element in the weld.

3 Results and discussion

3.1 FFR and Cr(VI) formation rate

The FFR (g/min) and hexavalent chromium formation rate (Cr(VI)FR) (mg/m^3) measured for the conventional and experimental electrodes are represented in Fig. 3. Here, C represents the conventional electrode comprising 100% natural rutile in its flux. With the addition of synthetic rutile to the flux, significant changes in FFR and Cr(VI)FR were detected. The electrode with 50% synthetic rutile in its flux exhibited a significant drop in FFR, up to 31.4% (E2). However, the subsequent addition of synthetic rutile raised the FFR in comparison to the test electrode (E2). Hexavalent chromium formation rate had exhibited a different trend in its variation. Initially, there was a significant reduction in Cr(VI)FR when 25% synthetic rutile was added to the electrode flux (E1). Further addition of synthetic rutile by 50% resulted in a modest rise in Cr(VI)FR, again followed by a

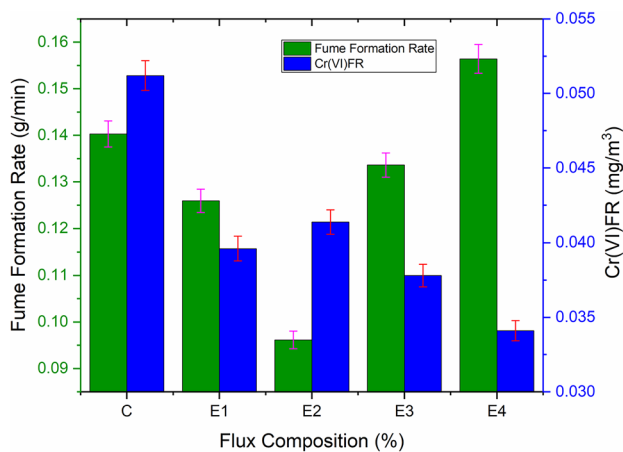


Fig. 3 Effect of flux composition on FFR and Cr(VI) formation rate. The error bars show the standard deviation of independent triplicate samples

decrease when 75% and 100% synthetic rutile was added to the flux. A careful examination of the preceding data indicates that, in order to achieve an acceptable reduction in both FFR and Cr(VI)FR, it would be advantageous to substitute 50% natural rutile in the flux with synthetic rutile (corresponding to the electrode E2). The following sections address the possible cause for FFR and Cr(VI)FR variation due to the presence of synthetic rutile in the flux.

3.1.1 Variation in fume formation rate

FFR is dependent of the arc stability. A stable arc is known to produce low fumes and vice versa. In order to get an estimate of the arc stability, the arc voltage probability density was plotted as a function of arc voltage as shown in Fig. 4. To ascertain the difference between the various rutile concentrations, certain portions of probability density plot (designated as a, b, and c in Fig. 4) were enlarged and highlighted.

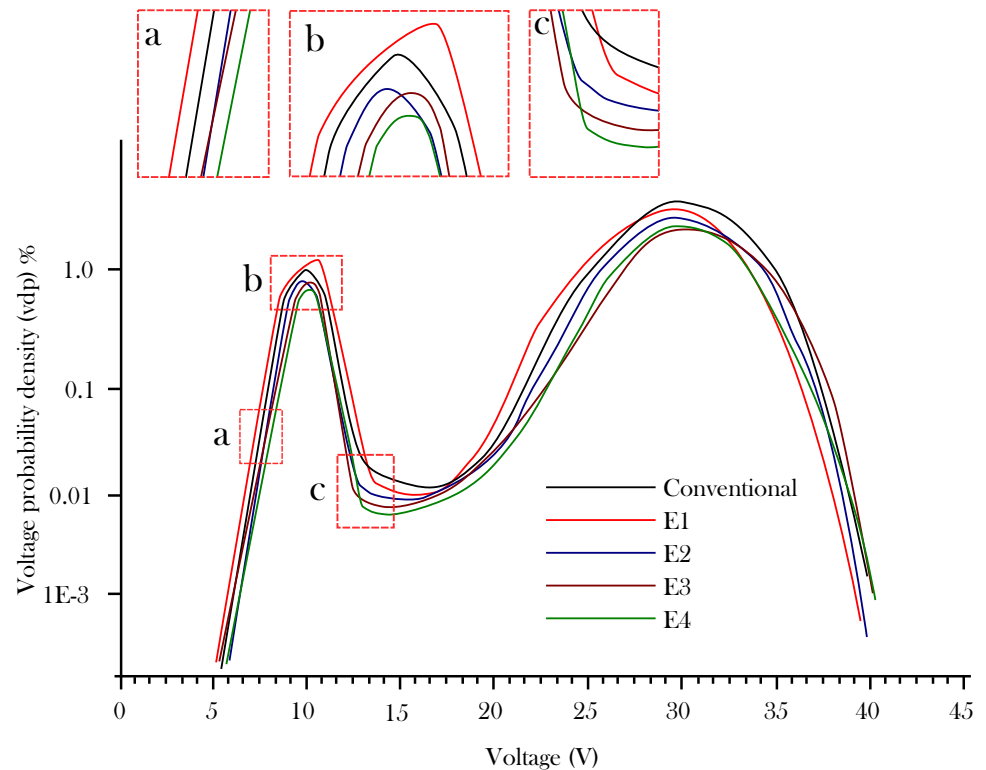
As can be observed, the probability density distribution of the arc voltage comprises two peaks with comparable shapes [26]. The smaller left-peak sector indicates increased arc stability. The integrated probability ΣU_S was computed by integrating the region of the left peak between the minimum and maximum voltages. Reduced ΣU_S (%) values indicate a reduced chance of short-circuit and explosion drop transfer, implying increased arc stability. The integrated probability density values of the conventional and experimental electrodes are shown in Table 3.

The combination E2 had the lowest ΣU_S value of 6.23%, indicating the highest arc stability among the tested electrodes, and justifies its low fume generation behavior, while E4 had a ΣU_S value of 7.69% close to that of the conventional electrode, indicating similar arc stability characteristics due to which their FFRs were also comparable.

Apart from arc stability, the droplet characteristics also decided the quantity of fumes generated. Figure 5 shows the variation in the size of the pendent liquid droplet as captured by a high-speed camera. It is obvious that the electrode E2 (with 50% synthetic rutile in its flux) had a smaller droplet diameter of 2.9 mm when compared with the conventional electrode (droplet diameter 4.2 mm) and other experimental electrodes. The considerable reduction in droplet diameter (by as much as 30%) could have ensued lower evaporation and hence a lower FFR. A close examination of Fig. 5d, e further reveals that the droplets from electrodes E3 and E4 were continuous and exhibited wandering effect resulting in splashing of the weld pool. This, in turn, might have resulted in higher fume levels.

The spatters formed from the electrodes were captured using infrared thermography as shown in Fig. 6 which clearly reveals a variation with the concentration of

Fig. 4 Probability density distribution of arc voltage during welding



synthetic rutile in the flux. The images were rendered at 300 frames per s, and the spatters observed in the images were highlighted with blue circles for better understanding. With an increase in the synthetic rutile flux concentration from 0 to 25% and to 50%, it was observed that the arc stability increased and attained a maximum stability at 50% of synthetic rutile flux addition. This is primarily associated with the differences in the droplet transfer characteristics (Fig. 5). For conventional electrodes, the pendent droplets were larger in size due to which, spatters will be generated upon detachment of droplets to the weld pool. With the addition of synthetic rutile up to 25%, the droplet size was found to reduce due to the reduced surface tension and pinching effect provided by the TiO_2 in the synthetic rutile. Hence, the spatter reduces for E1 compared to the conventional electrode C. The pinching effect was more pronounced with the 50% addition of synthetic rutile in the flux because of which the droplet size was further reduced

for E2 and the droplet transfer was finer and more stable than that of E1. Hence, the spatter density also reduced for E2. Subsequent addition of synthetic rutile up to 75% and 100% in the flux progressively increased the pinching effect and resulted in continuous transfer of droplets from the electrode to the weld pool. This resulted in higher splashing and wandering effects of the weld pool leading to increased generation of spatters.

The variations in arc stability, droplet sizes, and spatter formations were greatly influenced by the physical and chemical characteristics of the rutile flux compositions. There were notable variations in the physical and chemical properties of synthetic rutile compared to natural rutile, which suits its application in welding process. As far as physical properties are concerned, synthetic rutile particles are fine grained and porous in structure compared to natural rutile. The SEM images shown in Fig. 7 clearly indicate that synthetic rutile contains fine-grained TiO_2 particles of size 150–212 μm compared to natural rutile having 180–850- μm -sized TiO_2 particles and being relatively porous than natural rutile.

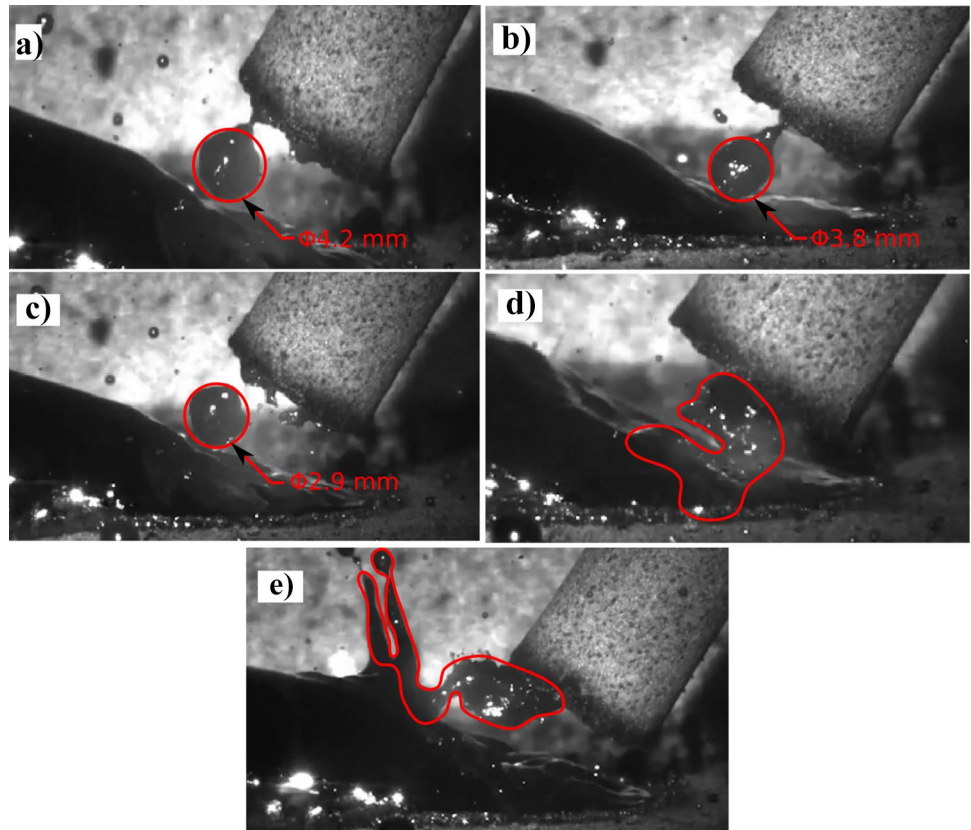
Yet, another difference in the physical property is the density of synthetic and natural rutilites. The electrode density was found decreasing with an increase in the concentration of synthetic rutile in the flux as shown in Table 4.

This trend is attributed to the lower density of synthetic rutile (2.3 g/cm^3) compared to natural rutile (4.23 g/cm^3). The variation in density of the electrode could be

Table 3 Integrated probability density

Particulars	Integrated probability (ΣU_s (%))
Conventional	7.34
E1	6.49
E2	6.23
E3	7.02
E4	7.69

Fig. 5 High-speed camera images showing droplet transfer from the **a** conventional electrode, **b** E1, **c** E2, **d** E3, and **e** E4



corroborated with its droplet transfer and fume generation behavior. A decrease in density would mean more quantity of synthetic rutile in a given volume of flux. As synthetic

rutile contains a rich content of fine-grained TiO_2 particles, its increase in concentration in the flux facilitates better reduction in surface tension of the pendent liquid droplet and

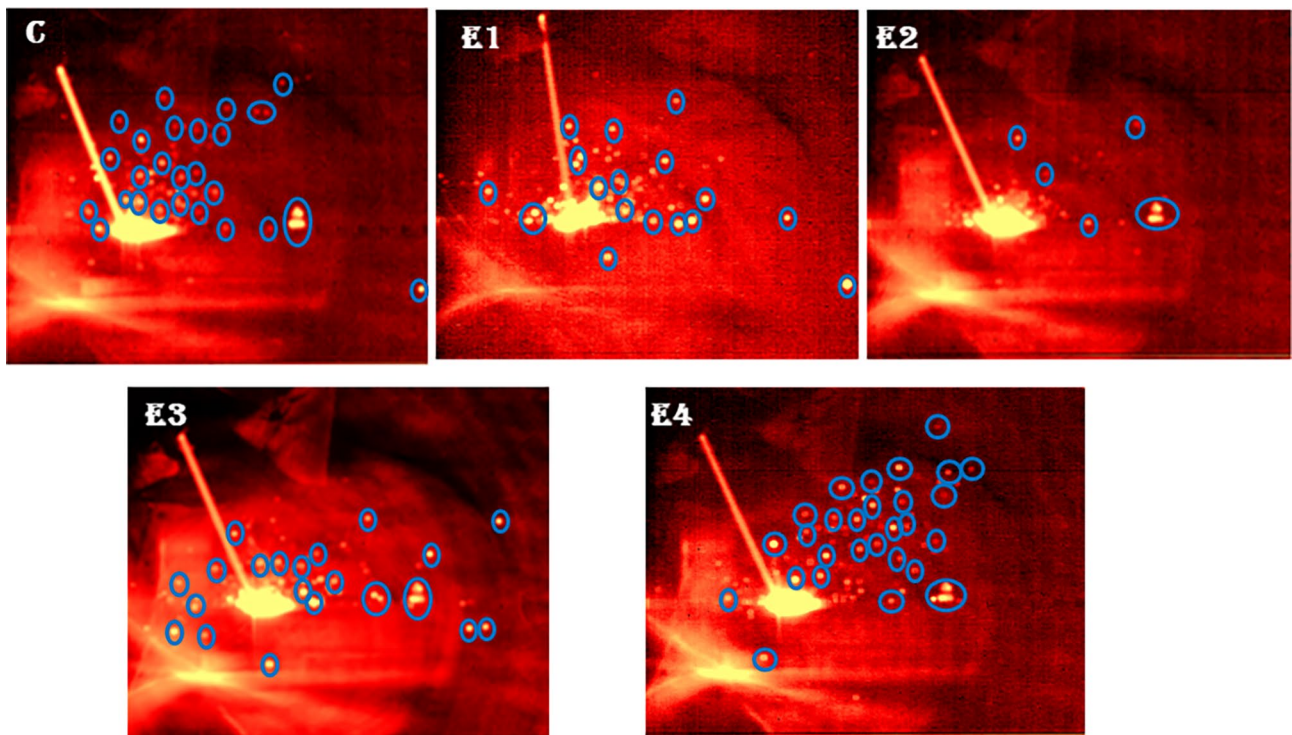


Fig. 6 Infrared camera images of spatter formation

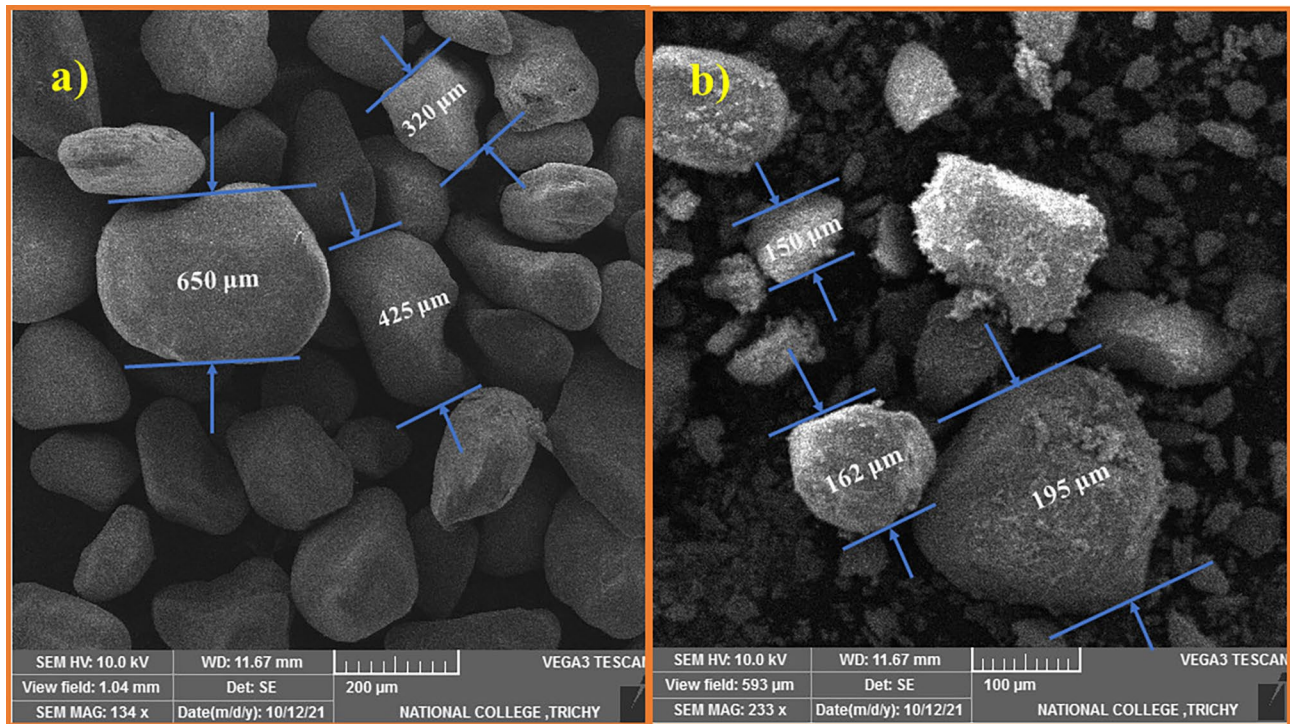


Fig. 7 a) SEM image of natural rutile. b) SEM image of synthetic rutile

hence promotes stable droplet transfer resulting in reduced fume levels [27].

Considering the chemical properties, there are significant differences in the chemical composition of natural and synthetic rutiles. The chemical composition of synthetic rutile and natural rutile as analyzed using XRF spectroscopy is given in Table 5.

As evident from the results, natural rutile contains 86.27% TiO_2 followed by elements such as Fe_2O_3 , SiO_2 , Al_2O_3 , CaO , MgO , and MnO . On the contrary, synthetic rutile assays 96.2% TiO_2 along with traces of other elements.

Hence, for a given quantity of flux, the involvement of TiO_2 on the droplet transfer behavior and hence on the reduction of fumes will be more prominent for synthetic rutile when compared to natural rutile.

3.1.2 Variation in hexavalent chromium formation rate

The effect of Zn on the Cr(VI) content in the welding fumes was analyzed. Cr(VI)FR varies with the UVC and ozone concentration in the weld atmosphere. When an amount of UVC

Table 4 Density of electrode coating

Electrode	Density (g/cm^3)
C	1.667
E1	1.555
E2	1.521
E3	1.501
E4	1.488

in the arc atmosphere increases, more reactive species of oxygen produced would react with normal oxygen molecule to form ozone as given in Eqs. (3) and (4) [28]. Furthermore, ozone, being unstable and a strong oxidizer, readily oxidizes the Cr(0) and Cr(III) to Cr(VI).



Figure 8 shows the plot of UVC radiation intensity, ozone, and Zn concentration for different flux compositions. The effect of flux modification on the intensity of UVC and ozone is apparent from this figure. Interestingly, two distinct trends could be observed in the figure. From conventional electrode to E1 (with 25% synthetic rutile in its flux), there was a trade-off between the UVC radiation and ozone. However, for E2 and other experimental electrodes (E3 and E4), the same linear relation between UVC and ozone (as mentioned in Eqs. (3) and (4)) could be observed. These variations might be attributed to the following reasons.

Apart from synthetic rutile, the experimental electrodes contain Zn, a reactive metal, in its flux formulation which readily oxidizes to ZnO fumes by reacting with the available oxygen free radical in the arc atmosphere as shown in Eq. (5).



This would deprive oxygen free radical for further reaction with O_2 (Eq. 4) and hence reduce the formation of ozone

Table 5 Chemical composition of natural and synthetic rutiles

Chemical composition							
	TiO ₂	Fe ₂ O ₃	MgO	CaO	SiO ₂	Al ₂ O ₃	MnO
Natural rutile	86.27	10.33	0.55	0.19	1.6	0.38	0.07
Synthetic rutile	96.2	3.01	0.14	0.11	0.31	0.054	0.02

in E1. Apparently, the Cr(VI)FR also reduced for E1. However, there was an increase in UVC radiation for E1. This might be attributed to the fact that the intensity of UVC radiation depends on the level of fumes in the arc atmosphere. A higher fume level would ensue a barrier effect for UVC radiation, minimizing its intensity in the arc atmosphere and vice versa [29]. The reason that E1 showed higher UVC than conventional electrode is due to its lower fume levels and hence reduced barrier effect.

For E2, with further addition of 50% synthetic rutile in the flux, there was a significant decrease in the generation of fumes compared to E1. The greater the reduction of fumes, the lesser the barrier effect which enables the reaction between UVC radiation and O₂ to form ozone in the arc atmosphere (Eqs. (3) and (4)). The higher concentration of ozone in the arc atmosphere might have caused a modest rise in Cr(VI)FR for E2 compared to E1. However, the Cr(VI)FR was still 20% less than the conventional electrode.

For electrodes E3 and E4, with 75% and 100% synthetic rutile in its flux, respectively, the UVC radiation and ozone were found to decrease which might possibly be attributed to the increase in generation of fumes. It is due to this reason that the Cr(VI)FR decreased for E3 and E4.

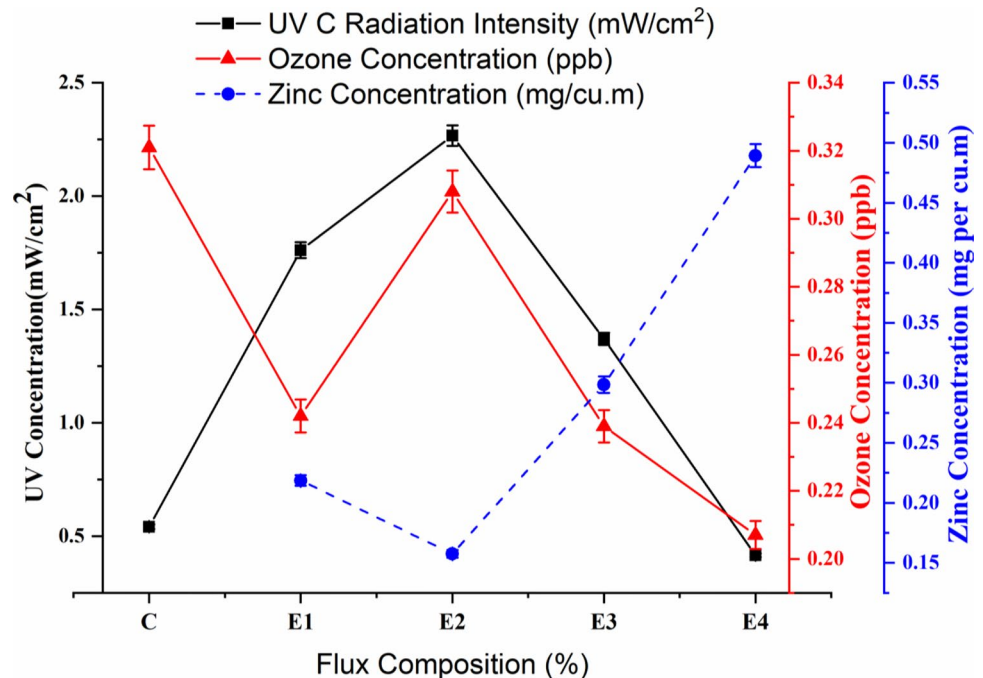
The variation in the concentration of Zn in fumes is also evident from Fig. 8. As can be noted from the figure, the

concentration of Zn in the fumes decreases from E1 to E2 and then increases for E3 and E4. Overall, the results indicate that Zn is effectively involved in ozone reduction only up to 25% addition of synthetic rutile to the flux. With an increase in the content of synthetic rutile, the effect of UVC in forming ozone was found to surpass the effect of Zn.

The constituent analysis shown in Fig. 9 also reveals that the electrode E2 had the lowest metallic constituent concentration except zinc, while for E4, it was the highest. This variation could be corroborated with the surface tension effect of the synthetic rutile. The enhanced pinching effect caused by an increase in surface tension have reduced the pendent liquid droplet size in E2 and hence its evaporation to fumes. Apart from this, the stable nature of the arc in E2 have favored alloying elements getting dragged to the weld pool (as evident from Table 6) and hence prevented it from oxidizing as fumes. However, for E3 and E4, there were increased wandering and splashing of the weld pool (Fig. 5) leading to higher oxidation and emission of the constituent elements in the arc atmosphere.

The above variation in metallic constituent concentration in fumes can be complemented by the results of the delta quantity analysis shown in Fig. 10. Delta quantity gives the amount of alloying elements recovered in the weld pool and is a direct indication of the quantity of

Fig. 8 Intensity of ozone and UV C formation for different flux composition. The error bars show the standard deviation of independent triplicate samples



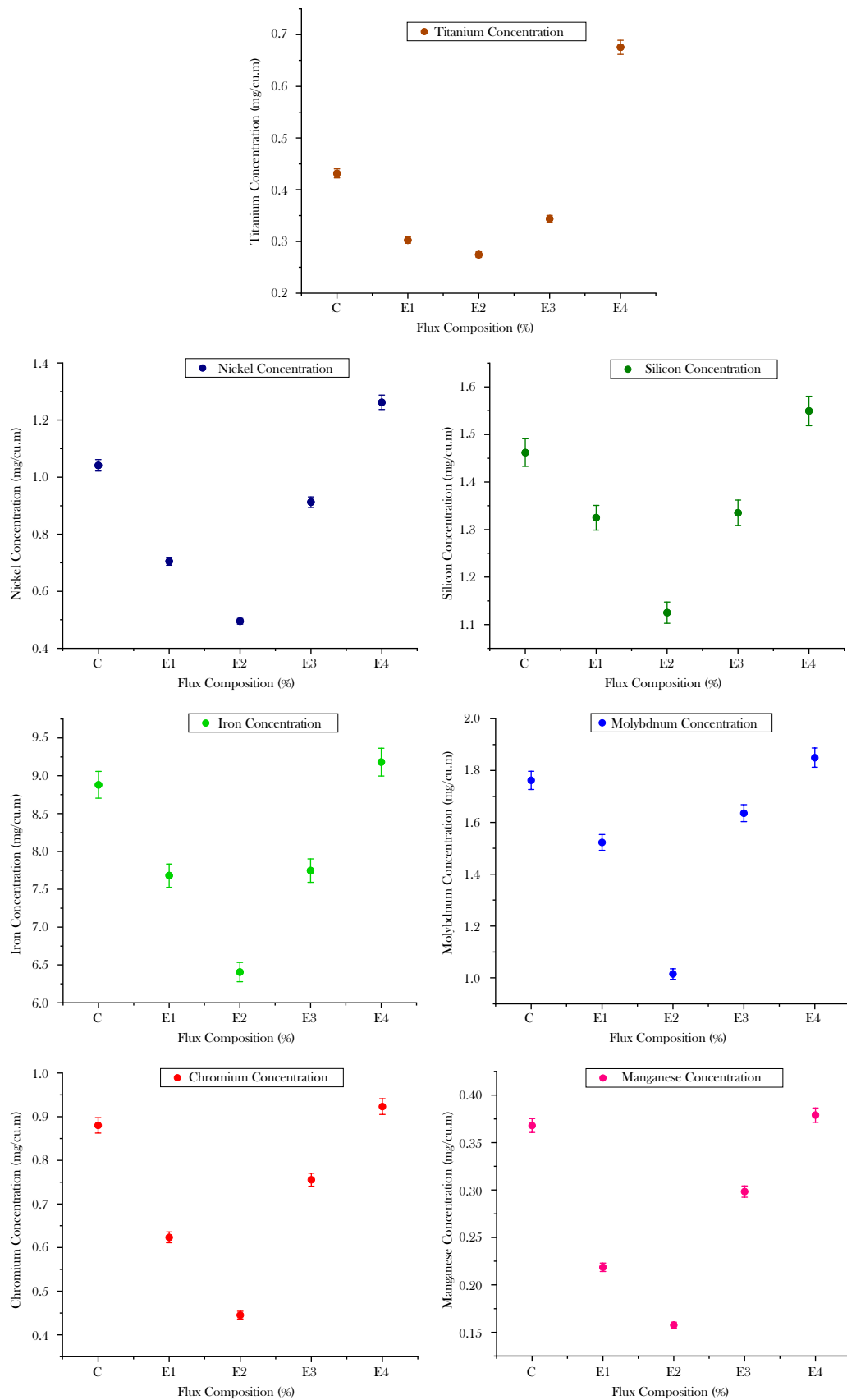


Fig. 9 Variation of different metallic constituent concentrations in different flux compositions. The error bars show the standard deviation of independent triplicate samples

Table 6 Chemical composition of weldments

Electrode identity	Chemical composition (wt%)					
	Cr	Mn	Fe	Ni	Si	Zn
C	18.21	0.95	66.43	11.23	0.99	–
E1	18.34	1.03	65.53	11.47	1.01	0.21
E2	18.44	1.13	65.97	11.90	1.2	0.42
E3	18.28	1.01	64.72	11.50	1.10	0.12
E4	18.19	0.93	64.40	10.95	0.97	0.05

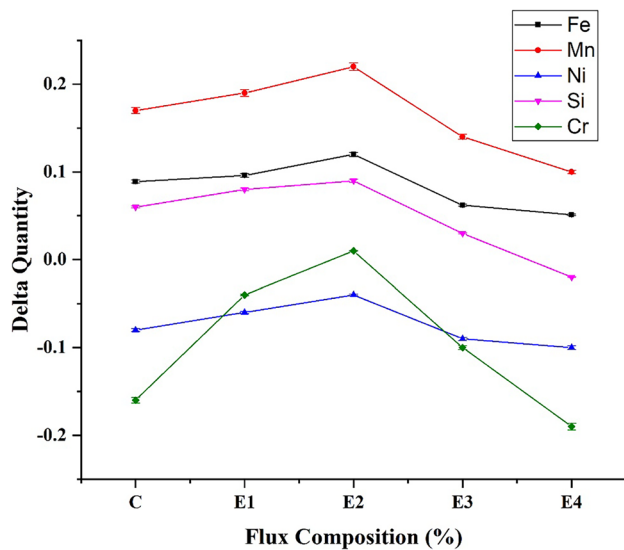


Fig. 10 Delta quantity analysis of the different combinations. The error bars show the standard deviation of independent triplicate samples

metals generated as fumes. It could be observed that the delta quantity was more positive for the electrode E2, indicating better transfer of alloying elements from the flux to the weld and hence a concomitant decrease in its availability for oxidation into fumes [30, 31]. The lower values of delta quantity of E3 and E4 (implying reduced deposition in the weldment) signify transfer of alloying elements to the slag followed by its evaporation into fumes.

4 Conclusions

Welding fume is an unwanted but unavoidable byproduct of arc welding process. This paper investigated the influence of introducing synthetic rutile and Zn to the electrode flux on its emission characteristics. The following conclusions could be made from the study:

- Fume generation rate varies with the quantity of synthetic rutile in the electrode flux. E2 containing 50% synthetic rutile in the flux showed up to 31.4% reduction in FFR than the conventional electrode.
- Moreover, the addition of Zn to the electrode flux had a significant effect on the intensity of UVC and ozone in the region of the arc, which affects the concentration of Cr(VI) production in the weld environment. E4 had the lowest UVC intensity, ozone concentration, and subsequent Cr(VI) concentration in the arc region compared to other experimental electrode compositions. In comparison, the E2 electrode generated a higher Cr(VI) FR value, but it was still 20% less than the conventional electrode.
- The enhanced pinching effect caused by an increase in the surface tension have reduced the pendent liquid droplet size in E2 and hence its evaporation to fumes. Thus, E2 was reported to have lower concentration of metallic elements such as Ti, Ni, Si, Fe, Mo, Cr, and Mn in fumes and was also found to have higher weld metal deposition than the conventional and other experimental electrodes.

Acknowledgements The authors would like to express their gratitude to the Director of the National Institute of Technology (NIT), Tiruchirappalli, for her unwavering encouragement and support throughout this endeavor. The authors would like to express their heartfelt gratitude to Cochin Minerals and Rutile Limited, Kerala, for supplying the raw materials necessary for the successful completion of this work.

Author contribution Rahul Madhusoodhanan: conceptualization, methodology, investigation, and writing of the original draft. Sivapirakasam Suthangathan Paramashivan: formal analysis, supervision, resources, and writing which included review and editing. Sreejith Mohan: methodology, validation, formal analysis, and investigation. Vishnu B. Rajeshwari: formal analysis and investigation. Guruvayurappan Murali: review and editing.

Availability of data and material Not applicable.

Code availability Not applicable.

Declarations

Ethics approval and consent to participate Not applicable.

Consent for publication All authors agreed to publish this manuscript in the *International Journal of Advance Manufacturing Technology* and confirmed that this work has not been published anywhere before.

Competing interests The authors declare no competing interests.

References

- MacLeod JS, Harris MA, Tjepkema M, Peters PA et al (2017) Cancer risks among welders and occasional welders in a national population-based cohort study: Canadian census health and environmental cohort. *Saf Health Work* 8(3):258–266
- Rissone NMR, Farias JP, Bott IS, Surian ES (2002) ANSI/AWS A5. 1–91 E6013 rutile electrodes: the effect of calcite. 113–124
- Zhang Y, Coetsee T, Yang H, Zhao T, Wang C (2020) Structural roles of TiO₂ in CaF₂-SiO₂-CaO-TiO₂ submerged arc welding fluxes. *Metall Mater Trans B* 51(5):1947–1952
- Akhgar BN, Pazouk M, Ranjbar M et al (2012) Application of Taguchi method for optimization of synthetic rutile nano powder preparation from ilmenite concentrate. *Chem Eng Res Des* 90(2):220–228
- Shojaei V, Schaffie M, Mohebbi A et al (2014) Upgrading of ilmenite using KOH sub-molten salt process assisted by mechanical activation. *Mater Manuf Process* 29(10):1284–1288
- Chen G, Ling Y, Li Q et al (2020) Highly efficient oxidation of Panzhihua titanium slag for manufacturing welding grade rutile titanium dioxide. *J Mater Res Technol* 9(4):7079–7086
- Sivapirakasam SP, Mohan S, Santhosh Kumar MC et al (2015) Welding fume reduction by nanoalumina coating on electrodes - towards green welding process. *J Clean Prod* 108:131–144
- Mohan S, Sivapirakasam SP, Santhosh Kumar MC et al (2015) Welding fumes reduction by coating of nano-TiO₂ on electrodes. *J Mater Process Technol* 219(May):237–247
- Sivapirakasam SP, Mohan S, Santhosh Kumar MC et al (2017) Control of exposure to hexavalent chromium concentration in shielded metal arc welding fumes by nano-coating of electrodes. *Int J Occup Environ Health* 23(2):128–142
- Vishnu BR, Sivapirakasam SP, Sathpathy KK et al (2018) Cr 6+ reduction in welding fumes by nano composite coatings on stainless steel manual metal arc welding electrodes. *Process Saf Environ Prot* 114:334–346
- Lunau FW (1967) Ozone in arc welding. *Ann Occup Hyg* 10(3):175–188
- Vishnyakov VI, Kiro SA, Ennan AA (2020) Reducing of UV radiation intensity, ozone concentration and fume formation in gas metal arc welding. *Aerosol Sci Eng* 4(3):192–199
- Chadyšiene R, Girgždys A (2009) Assessment of ultraviolet (UV) radiation from technical sources. *J Environ Eng Landsc Manag* 17(3):164–170
- Kudo Y, Sakasai A, Hamada K et al (2004) Mechanical tests on the welding part of SS316LN after heat treatment for Nb3Sn superconducting conductor. *J Nucl Mater* 329–333(1–3 Part A):634–638
- Kim JB, Sohn I (2014) Effect of alumina and extended basicity on the viscosity and structure in the TiO₂-MnO-Al₂O₃-8.64 ZrO₂-2.77 Na₂O welding flux system. *ISIJ Int* 54(3):657–663
- Kim JB, Sohn I (2014) Effect of SiO₂/Al₂O₃ and TiO₂/SiO₂ ratios on the viscosity and structure of the TiO₂-MnO-SiO₂-Al₂O₃ welding flux system. *ISIJ Int* 54(9):2050–2058
- Kim JB, Sohn I (2013) Influence of TiO₂/SiO₂ and MnO on the viscosity and structure in the TiO₂-MnO-SiO₂ welding flux system. *J Non-Cryst Solids* 379:235–243
- EN ISO Standard: ISO 15011-1:2009. Health and safety in welding and allied processes – Laboratory method for sampling fume and gases generated by arc welding – Part 1: Determination of emission rate and sampling for analysis of particulate fume. <https://www.iso.org/obp/ui/es/#iso:std:iso:15011:-1:ed-2:v1:en>. Accessed 29 Jul 2022
- Srinivasan K, Balasubramanian V (2011) Effect of surface tension metal transfer on fume formation rate during flux-cored arc welding of HSLA steel. *Int J Adv Manuf Technol* 56(1–4):125–134
- Okuno T, Ojima J, Saito H (2001) Ultraviolet radiation emitted by CO₂ arc welding. *Ann Occup Hyg* 45(7):597–601
- Dennis JH, Mortazavi SB, French MJ, Hewitt PJ et al (1997) The effects of welding parameters on ultraviolet light emissions, ozone and Cr(VI) formation in MIG welding. *Ann Occup Hyg* 41(1):95–104
- Liu HH, Wu YC, Chen HL (2007) Production of ozone and reactive oxygen species after welding. *Arch Environ Contam Toxicol* 53(4):513–518
- Fernandes R, van Os BJH, Huisman HDJ (2013) The use of hand-held XRF for investigating the composition and corrosion of Roman copper-alloyed artefacts. *Herit Sci* 1(1):1–7
- Zhang J, Coetsee T, Wang C (2020) Element transfer behaviors of fused CaF₂-SiO₂ fluxes subject to high heat input submerged arc welding. *Metall Mater Trans B* 51(1):16–21
- Zhang J, Coetsee T, Dong H, Wang C (2020) Element transfer behaviors of fused CaF₂-TiO₂ fluxes in EH36 shipbuilding steel during high heat input submerged arc welding. *Metall Mater Trans B* 51(5):1953–1957
- Vishnu BR, Sivapirakasam SP, Sathpathy KK, Albert SK, Chakraborty G (2018) Influence of nano-sized flux materials in the reduction of the Cr (VI) in the stainless steel welding fumes. *J Manuf Process* 34(March):713–720
- Bachmann B, Siewert E, Schein J (2012) In situ droplet surface tension and viscosity measurements in gas metal arc welding. *J Phys D Appl Phys* 45(17)
- Wang J, Kalivoda M, Guan J et al (2012) Double shroud delivery of silica precursor for reducing hexavalent chromium in welding fume. *J Occup Environ Hyg* 9(12):733–742
- Dennis JH, French MJ, Hewitt PJ, Mortazavi SB, Redding CAJ (2002) Control of occupational exposure to hexavalent chromium and ozone in tubular wire arc-welding processes by replacement of potassium by lithium or by addition of zinc. *Ann Occup Hyg* 46(1):33–42
- Almostaneer H, Cadigan C, Liu S, Olson DL, Richards R, Liang HJ (2011) Hydrocarbon-metal reactions during metal arc welding under oil (MAW-UO). *Sci Technol Weld Join* 16(7):619–629
- Zhang J, Leng J, Wang C (2019) Tuning weld metal mechanical responses via welding flux optimization of TiO₂ content: application into EH36 shipbuilding steel. *Metall Mater Trans B* 50(5):2083–2087

Publisher's note Springer Nature remains neutral with regard to jurisdictional claims in published maps and institutional affiliations.

Springer Nature or its licensor holds exclusive rights to this article under a publishing agreement with the author(s) or other rightsholder(s); author self-archiving of the accepted manuscript version of this article is solely governed by the terms of such publishing agreement and applicable law.